Electromagnetics: M F Iskander

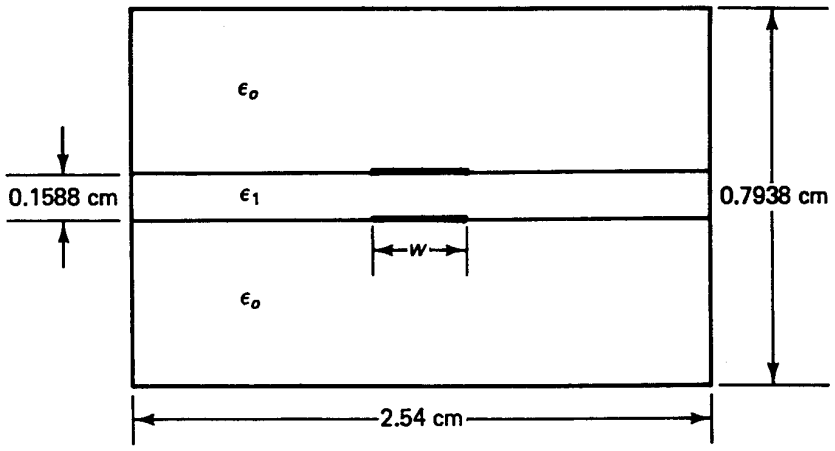

Figure 4.23 Geometry of strip capacitor.

the Gaussian contour to calculate the total charge, it is numerically preferred to take it along the finite difference mesh, midway between the center and outer conductors. After you write your program, you may compare your results with those given in Table 4.2, which illustrates the variation of C with the width of the center strip W and the dielectric constant ϵ_1.

TABLE 4.2 CAPACITANCE PER UNIT LENGTH pF/m FOR VARIOUS VALUES OF W AND ϵ_1

Strip width W (cm)	Teflon $\epsilon_r = 2.05$	Rexolite $\epsilon_r = 2.65$	Air
0.558	58.97	61.83	53.86
0.7145	67.62	70.51	62.34
0.8733	76.77	79.72	71.29

4.9 NUMERICAL SOLUTION OF ELECTROSTATIC PROBLEMS—METHOD OF MOMENTS

In section 4.3, we introduced the concept of electric potential and obtained integral equations that relate the potential to a given charge distribution. For example, if $\rho_s(\mathbf{r}')$ is a surface charge distribution, it is shown that $\Phi(\mathbf{r})$ is given by

$$\Phi(\mathbf{r}) = \frac{1}{4\pi\epsilon_o} \int_s \frac{\rho_s \, ds'}{|\mathbf{r} - \mathbf{r}'|} \tag{4.59}$$

where $|\mathbf{r} - \mathbf{r}'|$ is the distance from the charge distribution $\mathbf{r}'$ to the point $\mathbf{r}$ at which the potential Φ is to be evaluated. In all the examples we solved to illustrate the application of equation 4.59, we assumed the charge distribution in simple geometries and evaluated equation 4.59 to calculate Φ at specific locations. In many engineering problems, including the determination of capacitance of a system of conductors of complex geometry, the charge distribution is not known and instead the potentials of the

conductors are known. We wish to solve for the charge distribution in equation 4.59 from given potentials on conductors. To emphasize the importance of developing this numerical solution procedure, we reexamine the problem of determining the capacitance of a parallel plate capacitor discussed in example 4.7. It is shown that under the assumption of having infinitely large parallel plates, that is, the dimensions of the plates are much larger than the separation distance, we found that the capacitance is given by

$$C = \frac{\epsilon_o A}{d}$$

where the total separation between the plates $d = d_1 + d_2$ and the medium is assumed air $\epsilon_o = \epsilon_1 = \epsilon_2$. As the separation d increases, the parallel plate approximation becomes less and less accurate because of the fringing field effects. Figure 4.24 shows the variation in the capacitance C as a function of the separation distance d. It is shown that as d reaches the side length w of the square parallel plate capacitor, C becomes more than three times larger than C_o, which is based on the infinite parallel plate assumption. This is certainly a significant difference, and more care should therefore be taken in calculating C. The problem is if such a simplifying assumption is not used, it is difficult to relate the potential to the charge distribution in a straightforward manner. Instead, numerical solutions should be used. We will illustrate the method of moments solution procedure by solving the following examples.

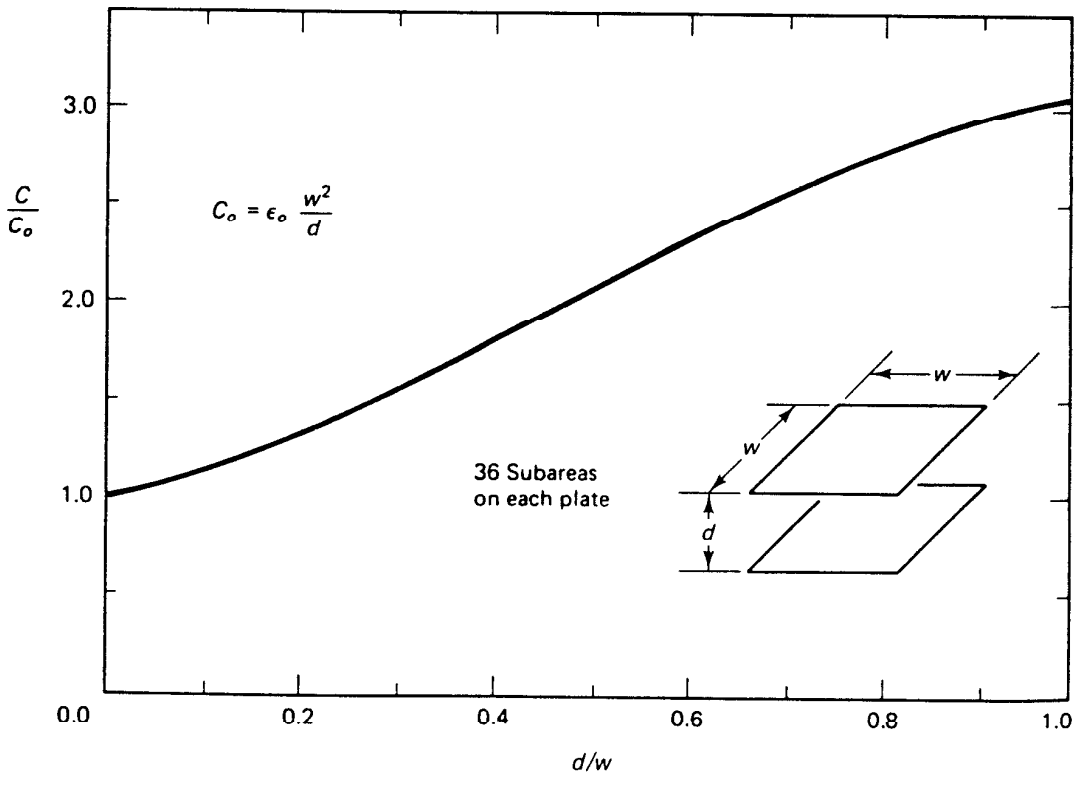

Figure 4.24 Variation of parallel plate capacitance with the increase of the separation distance d.

EXAMPLE 4.16

Consider a cylindrical conductor of radius a and length L. If the conductor is kept at a constant potential of 1 V, determine the charge distribution ρ_s on its surface.

Solution

The geometry of the cylindrical conductor is shown in Figure 4.25. The potential at any point $\mathbf{r}$ in space is related to the charge distribution $\rho_s(\mathbf{r}')$ by

$$\Phi(\mathbf{r}) = \frac{1}{4\pi\epsilon_o}\int_s \frac{\rho_s(\mathbf{r}')ds'}{|\mathbf{r}-\mathbf{r}'|} \tag{4.60}$$

To help us solve this problem numerically, we divide the conductor into N small sections. These sections are assumed to be sufficiently small so that the charge distribution is constant in each. Equation 4.60 then reduces to

$$\Phi(\mathbf{r}) = \frac{1}{4\pi\epsilon_o}\sum_{i=1}^{N} \frac{\rho_{si}\,\Delta s_i}{|\mathbf{r}-\mathbf{r}_i'|} \tag{4.61}$$

Figure 4.26 shows the sectioned conductor and total charge ($\rho_{si}\,\Delta s_i$) on each section. Equation 4.61 is an equivalent representation of the potential Φ at an observation point $\mathbf{r}$ owing to N point charges ($\rho_{si}\,\Delta s_i$) located at the center points ($\mathbf{r}_i'$) of the N sections. The surface area of each section is $\Delta s_i = 2\pi a\Delta\ell_i$, where $\Delta\ell_i = L/N$ is the length of each section. In equation 4.61, the N values of the charge density ρ_{si}, $i = 1, \ldots, N$ are unknown. In other words, equation 4.61 is one equation in the N unknown values of ρ_{si}. To determine these unknowns, we need N equations, which may be obtained by enforcing the validity of equation 4.61 at N points at which the potential Φ is known. Well, we know that $\Phi = 1$ V on the conductor. This means that $\Phi = 1$ V at the N centers of the sections. Therefore,

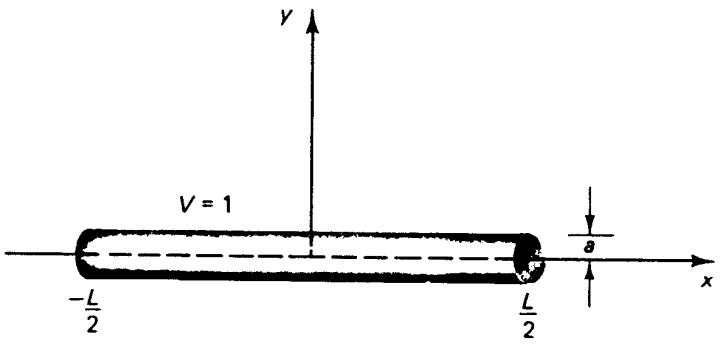

Figure 4.25 Geometry of straight conductor at potential $\Phi = 1$ V.

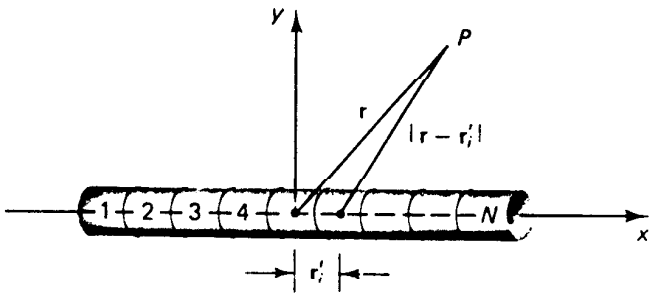

Figure 4.26 The potential at point P resulting from a point charge $\rho_{si}\,\Delta s_i$ located at the center of the ith section.

we may obtain the N desired equations by evaluating $\Phi = 1$ V at the N centers of the sections shown in Figure 4.26. Hence,

$$1 = \frac{1}{4\pi\epsilon_o}\left[\frac{\rho_{s1}\Delta s_1}{|x_1 - x_1|} + \frac{\rho_{s2}\Delta s_2}{|x_1 - x_2|} + \frac{\rho_{s3}\Delta s_3}{|x_1 - x_3|} + \cdots + \frac{\rho_{sN}\Delta s_N}{|x_1 - x_N|}\right]$$

$$1 = \frac{1}{4\pi\epsilon_o}\left[\frac{\rho_{s1}\Delta s_1}{|x_2 - x_1|} + \frac{\rho_{s2}\Delta s_2}{|x_2 - x_2|} + \frac{\nabla_{s3}\Delta s_3}{|x_2 - x_3|} + \cdots + \frac{\rho_{sN}\Delta s_N}{|x_2 - x_N|}\right]$$

$$\vdots$$

$$1 = \frac{1}{4\pi\epsilon_o}\left[\frac{\rho_{s1}\Delta s_1}{|x_N - x_1|} + \frac{\rho_{s2}\Delta s_2}{|x_N - x_2|} + \frac{\rho_{s3}\Delta s_3}{|x_N - x_3|} + \cdots + \frac{\rho_{sN}\Delta s_N}{|x_N - x_N|}\right] \tag{4.62}$$

In the set of N equations in equation 4.62, the first equation is obtained by enforcing the condition that $\Phi = 1$ V at the center x_1 (i.e., $\mathbf{r} = x_1$) of the first section. The second equation in equation 4.62 is obtained by enforcing $\Phi = 1$ V at the center x_2 of the second section. The charge $(\rho_{s1}\Delta s_1)$ is assumed to be located at the center x_1 of the first section, the charge $\rho_{s2}\Delta s_2$ is assumed located at the center x_2 of the second section, and so on. Equation 4.62 provides the desired N equations in the N unknown values of the charges $\rho_{s1}, \rho_{s2}, \ldots, \rho_{sN}$, assumed to be located at the center of the N sections.

Careful examination of equation 4.62, however, reveals that the self terms,

$$\frac{\rho_{s1}\Delta s_1}{|x_1 - x_1|}, \frac{\rho_{s2}\Delta s_2}{|x_2 - x_2|}, \frac{\rho_{s3}\Delta s_3}{|x_3 - x_3|}, \cdots, \frac{\rho_{sN}\Delta s_N}{|x_N - x_N|}$$

are singular. These terms result from calculating the potential Φ at the center of each section because of its own charge—that is, the source point $\mathbf{r}'$ and observation point $\mathbf{r}$ are the same. Solution for the set of equations in equation 4.62 is hence not possible, and some additional effort is required to remedy the singular behavior of the self terms. To do this, we examine closely the situation in the ith section shown in Figure 4.27. In the diagonal elements in equation 4.62, we were trying to evaluate the potential at the center of each section resulting from its own charge, which is also assumed to be located at the center of the section. To overcome the singularity problem, therefore, we do not assume that the charge is located at the center but instead distributed at the surface of the conductor. This is actually the situation to begin with, and what resulted in the singularity is our desire to use the point charges approximation in equation 4.61. From Figure 4.27, we may evaluate the potential at the center x_i of the ith cell as

$$\Phi = 1 = \frac{1}{4\pi\epsilon_o}\int_{-\Delta\ell_i/2}^{\Delta\ell_i/2}\int_0^{2\pi}\frac{\rho_{si}\, a\, d\phi\, dx'}{\sqrt{a^2 + x'^2}} \tag{4.63}$$

In equation 4.63, the distance from the charge point on the surface to the observation point at the center is taken $|\mathbf{r} - \mathbf{r}'| = \sqrt{a^2 + x'^2}$. Integrating equation 4.63, we obtain

$$1 = \frac{1}{4\pi\epsilon_o}\rho_{si}(2\pi a)\, \ell n\left[x' + \sqrt{a^2 + x'^2}\right]\Bigg|_{-\Delta\ell_i/2}^{\Delta\ell_i/2}$$

$$= \frac{\rho_{si}\, a}{2\epsilon_o}\, \ell n \frac{\frac{\Delta\ell_i}{2} + \sqrt{a^2 + \left(\frac{\Delta\ell_i}{2}\right)^2}}{-\frac{\Delta\ell_i}{2} + \sqrt{a^2 + \left(\frac{\Delta\ell_i}{2}\right)^2}}$$

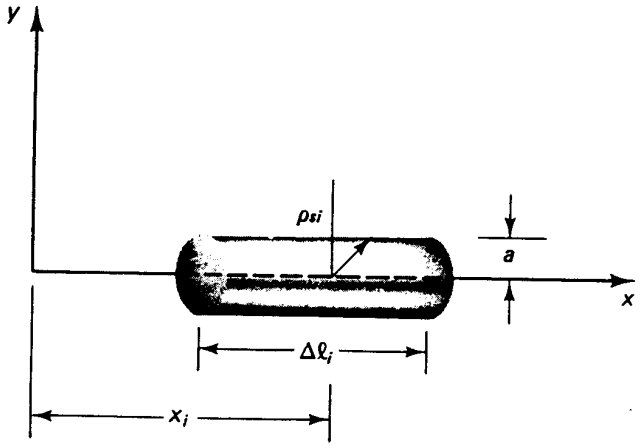

Figure 4.27 The potential at the center of the ith section resulting from its own surface charge.

For a conductor of small radius as compared to the length $\Delta\ell_i$ of each section, we obtain

$$1 = \frac{\rho_{si}\, a}{2\epsilon_o} \ell n \frac{\Delta\ell_i}{-\frac{\Delta\ell_i}{2} + \frac{\Delta\ell_i}{2}\left[1 + \frac{1}{2}\frac{a^2}{\left(\frac{\Delta\ell_i}{2}\right)^2}\right]}$$

$$= \frac{\rho_{si}\, a}{\epsilon_o} \ell n \frac{\Delta\ell_i}{a} \tag{4.64}$$

Equation 4.64 may be used for the diagonal (self) terms in equation 4.62, thus resulting in the following matrix equation:

$$\begin{bmatrix} 4\pi\epsilon_o \\ 4\pi\epsilon_o \\ 4\pi\epsilon_o \\ \vdots \\ 4\pi\epsilon_o \end{bmatrix} = \begin{bmatrix} 4\pi a\, \ell n \frac{\Delta\ell_1}{a} & \frac{2\pi a\,\Delta\ell_2}{|x_1 - x_2|} & \frac{2\pi a\,\Delta\ell_3}{|x_1 - x_3|} & \cdots & \frac{2\pi a\,\Delta\ell_N}{|x_1 - x_N|} \\ \frac{2\pi a\,\Delta\ell_1}{|x_2 - x_1|} & 4\pi a\, \ell n \frac{\Delta\ell_2}{a} & \frac{2\pi a\,\Delta\ell_3}{|x_2 - x_3|} & \cdots & \frac{2\pi a\,\Delta\ell_N}{|x_2 - x_N|} \\ \frac{2\pi a\,\Delta\ell_1}{|x_3 - x_1|} & \frac{2\pi a\,\Delta\ell_2}{|x_3 - x_2|} & 4\pi a\, \ell n \frac{\Delta\ell_3}{a} & \cdots & \frac{2\pi a\,\Delta\ell_N}{|x_3 - x_N|} \\ \frac{2\pi a\,\Delta\ell_1}{|x_N - x_1|} & \frac{2\pi a\,\Delta\ell_2}{|x_N - x_2|} & \frac{2\pi a\,\Delta\ell_3}{|x_N - x_3|} & \cdots & 4\pi a\, \ell n \frac{\Delta\ell_N}{a} \end{bmatrix} \begin{bmatrix} \rho_{s1} \\ \rho_{s2} \\ \rho_{s3} \\ \\ \rho_{sN} \end{bmatrix} \tag{4.65}$$

Equation 4.65, which can be further simplified if we choose all the sections of the same length $\Delta\ell_1 = \Delta\ell_2 = \cdots = \Delta\ell_N$, may now be solved by a simple matrix inversion subroutine. The result is the charge distribution $\rho_{s1}, \rho_{s2}, \ldots, \rho_{sN}$ on the surface of the conductor.

Exercise

Write a computer program that solves for the charge distribution on the surface of a conductor of radius a and length L. In addition to the geometry of the conductor, the input to the program should include the number of sections and the dielectric properties

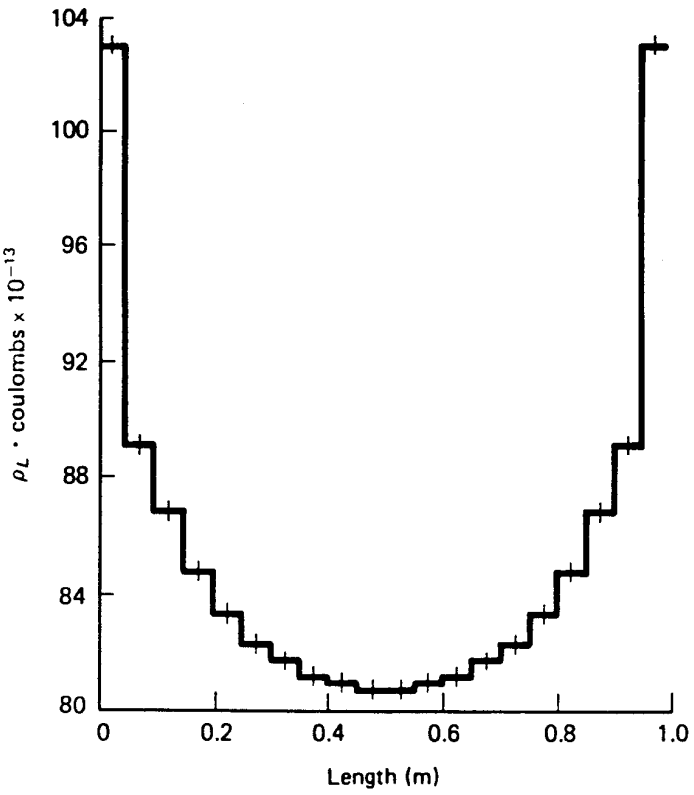

Figure 4.28 Charge distribution on a cylindrical conductor of radius $a = 1$ mm and length $L = 1$ m. The conductor is at a potential of 1 V. (See L. L. Tsai and C. E. Smith, Moment Method in Electromagnetics for Undergraduates, IEEE Trans. on Education, vol. E-21, pp. 14–22, 1979)

ϵ of the surrounding medium. Check your results with those shown in Figure 4.28 for a conductor of radius $a = 1$ mm and of length $L = 1$ m. The conductor is at a potential of 1 V, and twenty sections were used to obtain the results shown in Figure 4.28.

One may wonder if it was really worth going through all of this to determine the charge distribution on the surface of a cylindrical conductor. The answer is that although it seems too much effort for this simple geometry, the method of moment solution procedure is general and certainly capable of handling much more complicated conductor geometries at no additional effort than what we spent in the last example. The large variation of the charge distribution on the conductor as shown in Figure 4.28 also justifies the spent effort. Many of the electrostatic problems at the end of this chapter cannot be handled using rigorous solution procedures, and use of numerical ones such as the method of moment is appropriate. The following example will illustrate the application of the method of moment to multiconductor problems.

EXAMPLE 4.17

Consider the parallel plate capacitor shown in Figure 4.29a. We wish to use the method of moments to determine the capacitance as a function of the separation distance between the parallel plates.